Fundamental Properties of Eigenstate Wave Functions of $\mathcal{PT}$–Symmetric Anharmonic Oscillators

J. H. Noble[1] and U. D. Jentschura[1,2]

[1] *Department of Physics, Missouri University of Science and Technology, Rolla, Missouri 65409, USA*
[2] *MTA–DE Particle Physics Research Group, P.O.Box 51, H-4001 Debrecen, Hungary*

arXiv:1301.5758v1 [quant-ph] 24 Jan 2013

The $\mathcal{PT}$-symmetric cubic oscillator with Hamiltonian $H_3 = -\frac{1}{2}\,\partial_x^2 + \frac{1}{2}x^2 + \mathrm{i}\,G\,x^3$ is a paradigmatic example of a pseudo-Hermitian, or $\mathcal{PT}$-symmetric Hamiltonian with a purely real spectrum when endowed with $L^2(\mathbb{R})$ boundary conditions. Eigenfunctions of the stationary Schrödinger equation $H_3\,\psi_n(x) = E_n\,\psi_n(x)$ are manifestly complex, while the energy eigenvalues E_n are real and positive. Although H_3 does not commute with the parity operator, we find that for a natural choice of the global complex phase of the eigenstate wave function, the real and imaginary parts of the eigenfunctions [i.e., $\mathrm{Re}\,\psi_n(x)$ and $\mathrm{Im}\,\psi_n(x)$] are eigenstates of parity. Both the real and imaginary parts of the eigenfunctions are found to have an infinite number of zeros, even for the ground state and even for infinitesimal G, but the real and imaginary parts of $\psi_n(x)$ never vanish simultaneously when $G > 0$. Furthermore, we find that the eigenfunctions are "concentrated" in an "allowed" region where the energy E_n is larger than the complex modulus of the complex potential. $\mathcal{PT}$-symmetric Hamiltonians constitute natural generalizations of Hermitian Hamiltonians as time-evolution operators. Our results suggest that $\mathcal{PT}$-symmetric (pseudo-Hermitian) time evolution can naturally be interpreted as time evolution in a situation where manifestly complex "gain" and "loss" terms mutually compensate and lead to the real energy eigenvalues.

PACS numbers: 03.65.Ge, 02.60.Lj, 11.15.Bt, 11.30.Er

I. INTRODUCTION

Quantum mechanics promotes a number of physical quantities, which are purely real in classical physics, into the complex domain. An example is the momentum which is a real, measurable physical quantity in classical physics, but its quantum mechanical equivalent, the momentum operator $\vec{p} = -\mathrm{i}\,\vec{\nabla}$, contains the imaginary unit. A quantum mechanical wave function $\psi(\vec{r})$ is manifestly complex. Plane-wave eigenstates of the free Schrödinger Hamiltonian $H_0 = -\vec{\nabla}^2/(2m)$ also are eigenstates of the momentum operator $\vec{p} = -\mathrm{i}\vec{\nabla}$ and are of the form $\exp(\mathrm{i}\,\vec{k}\cdot\vec{r})$. A purely real eigenfunction such as $\cos(\vec{k}\cdot\vec{r})$ does not describe a particle with definite momentum.

Yet, under special circumstances, it is possible to construct eigenfunctions of operators which are purely real. Indeed, it is known [1, 2] that the eigenfunctions of the harmonic oscillator can be chosen as purely real functions, and furthermore, eigenfunctions of the quartic anharmonic one-dimensional oscillator

$$H_4 = -\frac{1}{2}\,\partial_x^2 + \frac{1}{2}\,x^2 + g\,x^4\,, \qquad g > 0\,, \tag{1}$$

can also be chosen as purely real. Here, we assume that H_4 is endowed with $L^2(\mathbb{R})$ boundary conditions. This implies that the wave function vanishes at infinity, i.e., $\psi(x) \to 0$ for $x \to \pm\infty$.

It has recently been observed [3–7] that the Hamiltonian

$$H_3 = -\frac{1}{2}\,\partial_x^2 + \frac{1}{2}\,x^2 + \mathrm{i}\,G\,x^3\,, \qquad G > 0\,, \tag{2}$$

has a real spectrum when endowed with $L^2(\mathbb{R})$ boundary conditions. The Hamiltonian H_3 commutes with the combined parity-time-reversal operator, $[\mathcal{P}\,\mathcal{T}, H_3] = 0$. Here, $\mathcal{P}$ is the parity $x \to -x$, and $\mathcal{T}$ is the time reversal, which for H_3 amounts to the replacement $\mathrm{i} \to -\mathrm{i}$. Operators with these properties have been analyzed recently [3, 8] and have been advocated as viable alternatives to Hermitian operators. The $\mathcal{PT}$-symmetry property implies that

$$H_3 = \mathcal{P}\;\mathcal{T}\;H_3\;\mathcal{T}\;\mathcal{P} = \mathcal{P}\;H_3^+\;\mathcal{P}\,, \tag{3}$$

where H_3^+ is the Hermitian adjoint. Here, we have used the relation $\mathcal{P}^2 = \mathcal{T}^2 = 1$ and thus $(\mathcal{PT})^{-1} = \mathcal{T}\,\mathcal{P}$.

If a Hamiltonian H fulfills a relation of the type $H = \eta^{-1}\,H^+\,\eta$, then H is said to be pseudo-Hermitian [9]. Here, following Pauli [9], we only require the metric operator η to be Hermitian. The Hermitian adjoint H^+ is calculated as $H^+ = \mathcal{T}\,H\,\mathcal{T}$, and thus, $\mathcal{PT}$-symmetry is identified as a special case of pseudo-Hermiticity ($\eta = \mathcal{P}$). One can generically show [9] that the scalar product

$$\langle\psi(t)|\phi(t)\rangle_* \equiv \int \mathrm{d}x\,\psi^*(t,x)\mathcal{P}\phi(t,x) \tag{4}$$

is conserved under time evolution if both ψ and ϕ fulfill the time-dependent Schrödinger equation $\mathrm{i}\partial_t\psi(t) = H_3\psi(t)$, and $\mathrm{i}\partial_t\phi(t) = H_3\phi(t)$. However, the integrand in Eq. (4) is manifestly "nonlocal" because $\psi^*(t,x)\mathcal{P}\phi(t,x) = \psi^*(t,x)\phi(t,-x)$; it depends on functions evaluate at x and $-x$.

In the prolific literature on $\mathcal{PT}$-symmetric quantum mechanics (see Refs. [3, 5, 6, 8–18] for an incomplete list), the spectrum of $\mathcal{PT}$-symmetric Hamiltonians has been analyzed in detail. However, much less attention has been devoted to the wave functions corresponding to the eigenstates. An analysis of the wave functions appears indicated because a number of interesting field-theoretical

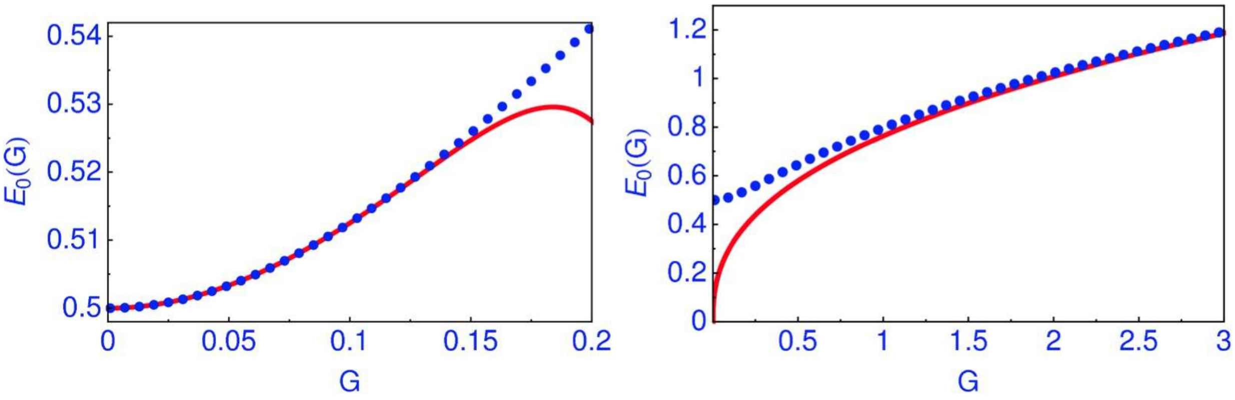

(a)

(b)

FIG. 1: (Color online.) The ground-state energy of the anharmonic oscillator Hamiltonian with imaginary cubic perturbation, as given in Eq. (2), is plotted in the perturbative (weak-coupling) regime in Fig. (a). The solid curve represents the results from eighth-order perturbation theory (terms up to the order G^8). In Fig. (b), the same eigenvalue is plotted in the strong-coupling regime $G > 0$. The small dots represent numerical values.

model theories and a streamlined description of phenomenologically important so-called $\mathcal{PT}$-symmetric wave guides rely on $\mathcal{PT}$-symmetric quantum mechanics and field theory (a brief overview is provided in Appendix A). Moreover, the concept of a $\mathcal{PT}$-symmetric Hamiltonian has recently been instrumental the Bender–Wu formulas [19–21] for odd anharmonic oscillators [5, 6]. It is self-evident that an improved intuitive understanding of the physics involved in $\mathcal{PT}$-symmetric models requires further understanding of the wave functions.

With reference to the wave functions, the following question is of interest: The Hamiltonian H_3 given in Eq. (2) involves a manifestly complex potential, which we denote as $W(x)$,

$$W(x) = \frac{1}{2}\,x^2 + \mathrm{i}\,G\,x^3 = V(x)\,\mathrm{e}^{\mathrm{i}\,\arg(V(x))}\,, \tag{5a}$$

$$V(x) = |W(x)| = \sqrt{\tfrac{1}{4}\,x^4 + G^2\,x^6}\,. \tag{5b}$$

The complex modulus $V(x) = |W(x)|$ tends to infinity as $x \to \pm\infty$. For purely real potentials like the "confining" quartic oscillator given in Eq. (1), intuition suggests that the "bulk" of the probability density of the eigenstate wave function should be concentrated in the "classically allowed" region, i.e., in the region where the eigenenergy E is greater than the potential, i.e., $E > V(x)$ [where $V(x) \in \mathbb{R}$]. The generalization of this concept to $\mathcal{PT}$-symmetric quantum mechanics needs to be clarified. For a manifestly complex potential, the condition $E > W(x)$ [with $W(x) \in \mathbb{C}$] cannot be applied because the complex numbers are not ordered.

The quartic anharmonic oscillator Hamiltonian given in Eq. (1) commutes with parity. By contrast, the eigenstate wave functions of a $\mathcal{PT}$-symmetric Hamiltonian do not need to be eigenstates of parity, because the parity operator does not commute with the $\mathcal{PT}$-symmetric Hamiltonian. These observations raise a number of obvious pertinent questions which we aim to address. We proceed by recalling a few basic facts about eigenvalue perturbation theory in Sec. II, analyzing the parity of eigenstates in Sec. III, and continue with a visualization of the manifestly complex $\mathcal{PT}$-symmetric eigenstates in Sec. IV. This leads to a generalization of the "classically allowed" region to the $\mathcal{PT}$-symmetric domain. We conclude the discussion in Sec. V.

II. ASYMPTOTICS OF IMAGINARY CUBIC PERTURBATION

In order to fix ideas, we first recall a few basic facts about eigenvalue perturbation theory and the imaginary cubic perturbation. One can split the Hamiltonian given in Eq. (2) into an unperturbed harmonic-oscillator term $H^{(0)} = -\frac{1}{2}\,\partial_x^2 + \frac{1}{2}\,x^2$ and a perturbation $H^{(1)} = \mathrm{i}\,G\,x^3$. Starting from the unperturbed harmonic oscillator eigenvalues $H^{(0)}|n\rangle = \epsilon_n^{(0)}|n\rangle$, where $\epsilon_n^{(0)} = n + \frac{1}{2}$, one can develop perturbation theory for the eigenvalues ϵ_n of $H_3 = H^{(0)} + H^{(1)}$, either using the classical Rayleigh–Schrödinger approach [2] or using a complex contour integration of the logarithm of the wave function (Riccati equation, see Refs. [22, 23]). The first nonvanishing term in perturbation theory is of second order and reads as

$$\epsilon_n^{(2)} = -\sum_{m \neq n} \frac{\langle m|H^{(1)}|n\rangle\langle n|H^{(1)}|m\rangle}{\epsilon_m^{(0)} - \epsilon_n^{(0)}} \tag{6a}$$

$$= G^2 \sum_{m \neq n} \frac{\left|\langle m|x^3|n\rangle\right|^2}{m - n} \tag{6b}$$

$$= \frac{G^2}{8}\left(30n^2 + 30n + 11\right) + \mathcal{O}(G^4)\,, \tag{6c}$$

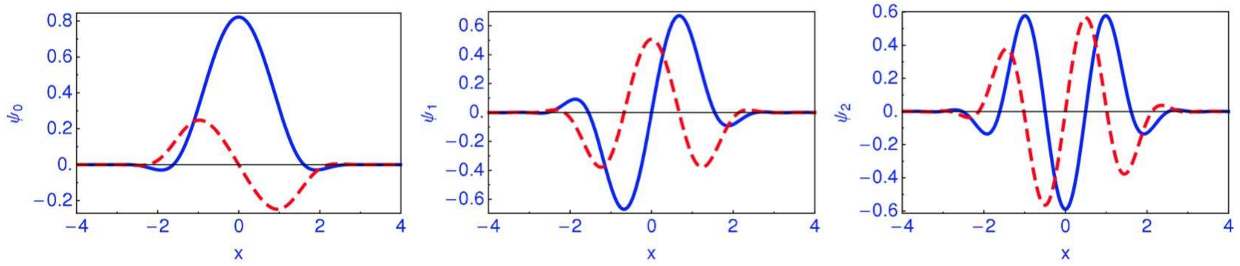

(a) (b) (c)

FIG. 2: (Color online.) Figure (a) displays the ground-state wave function of the imaginary cubic Hamiltonian (2) for $G = 1.0$. This wave function is manifestly complex. The real part $\mathrm{Re}\,\psi_0(x)$ (even under parity) is plotted using solid lines, and the dashed curve corresponds to the parity-odd imaginary part $\mathrm{Im}\,\psi_0(x)$. For the first excited state (still, $G = 1.0$), the real part is odd, while the imaginary part is even under parity [see Fig. (b)]. The second excited state [Fig. (c)] has an even real part, while its imaginary part is odd. The global complex phase of the wave function is chosen so that the real part $\mathrm{Re}\,\psi_{n=0,1,2}(x)$ of the wave functions has the same qualitative behavior as the eigenstate wave function of the quartic oscillator displayed in Fig. 4(a).

so that $\epsilon_n \approx \epsilon_n^{(0)} + \epsilon_n^{(2)}$. There is an observation to be made: Unlike for any second-order perturbation involving a Hermitian operator, the second-order term here is positive and shifts the ground-state energy level upward instead of downward. Through fourth order, the result reads as

$$\begin{aligned}\epsilon_n \sim n + \frac{1}{2} + \frac{G^2}{8}\left(30n^2 + 30n + 11\right) \\ - \frac{15}{32}\, G^4 \,\left(94n^3 + 141n^2 + 109n + 21\right) + \mathcal{O}(G^6))\,,\end{aligned} \tag{7}$$

where n is the principal quantum number. For the ground state ($n = 0$), this expression evaluates to $1/2 + 11\,G^2/8 - 465\,G^4/32$, while going to eighth order we obtain $1/2 + 11\,G^2/8 - 465\,G^4 + 39709\,G^6/128 - 19250805\,G^8/2048$ which is plotted against numerical values of the ground-state energy in Fig. 1(a). The positive curvature of the ground-state energy in the weak-coupling regime is clearly visible.

We can also look at the strong-coupling asymptotic as $G \to \infty$, for which we employ the "poor man's scaling" $x \to G^{-2/5}x$. The Hamiltonian H_3 is thus replaced by H_3', which has the same spectrum as H_3,

$$H_3' = G^{\frac{2}{5}}\left(-\frac{1}{2}\partial_x^2 + \mathrm{i}x^3 + \frac{1}{2}G^{-\frac{2}{5}}x^2\right)\,. \tag{8}$$

For large G, the eigenvalues ϵ_n of H_3' therefore go as

$$\epsilon_n \sim G^{\frac{2}{5}}\,\widetilde{\epsilon}_n\,, \qquad G \to \infty\,. \tag{9}$$

Here, the $\widetilde{\epsilon}_n$ are the energy eigenvalues of the Hamiltonian $\widetilde{H}_3$, with

$$\widetilde{H}_3 = -\frac{1}{2}\partial_x^2 + \mathrm{i}x^3 \to 2^{-\frac{3}{5}}\left(-\partial_x^2 + \mathrm{i}x^3\right)\,. \tag{10}$$

Indeed, the $\mathcal{PT}$-symmetric Hamiltonian $\widetilde{H}_3$ has its own set of eigenvalues, which we label as $\widetilde{\epsilon}_n$. In the last replacement step in Eq. (10), we have done the scaling transformation $x \to 2^{-\frac{1}{5}}\,x$. This transformation allows us to connect the strong-coupling asymptotics with the literature, notably, with Refs. [3] and [4, 7]. In particular, we have $\widetilde{\epsilon}_n = 2^{-\frac{3}{5}}\,E_n$ where the E_n are the energies of the Hamiltonian $-\partial_x^2 + \mathrm{i}x^3$.

III. PARITY OF EIGENSTATES

We have determined, to high numerical accuracy, the manifestly complex wave functions of the ground state and the first three excited eigenstates of the imaginary cubic oscillator (see Fig. 2). Because the parity operator $\mathcal{P}$ does not commute with the Hamiltonian H_3, the eigenstates of H_3 are not eigenstates of parity. Furthermore, because the potential is manifestly complex, so are the wave functions. Yet, numerical evidence drawn from Fig. 2 suggests that individually, both real as well as imaginary part of the eigenstate wave functions are eigenstates of parity. Eigenfunctions of a quantum Hamiltonian are only defined up to a global phase factor exp)(iφ) (and a dilation factor, in the sense of "rays" in Hilbert space)). The above statement therefore needs to be qualified: It holds if we perform the numerical diagonalization of the Hamiltonian (2) in a basis of harmonic-oscillator eigenfunctions.

We can formally split the Hamiltonian H_3 into a "real part" and a "imaginary part" as follows,

$$\mathrm{Re}\,H_3 = -\tfrac{1}{2}\,\partial_x^2 + \tfrac{1}{2}x^2\,, \tag{11a}$$

$$\mathrm{Im}\,H_3 = \mathrm{i}\,G\,x^3\,. \tag{11b}$$

If we also split the eigenstate wave function $\psi_n(x)$ into real and imaginary parts,

$$\psi_n(x) = \mathrm{Re}\,\psi_n(x) + \mathrm{i}\,\mathrm{Im}\,\psi_n(x)\,, \tag{12}$$

then it is rather easy to show, based on the decomposition (11), that if $\mathrm{Re}\,\psi_n(x)$ is even under parity and

$\psi_n(x)$ is an eigenstate of H_3 with real eigenvalue of ϵ_n, then $\mathrm{Im}\,\psi_n(x)$ has to be parity-odd, and vice versa. Also, if $\mathrm{Re}\,\psi_n(x)$ is odd under parity and $\psi_n(x)$ and the corresponding eigenvalue ϵ_n, is real, then $\mathrm{Im}\,\psi_n(x)$ has to be even under parity.

In Ref. [24], it has been observed that since $\mathcal{PT}$ commutes with the Hamiltonian, the eigenfunctions of H_3 also have to be eigenfunctions of the $\mathcal{PT}$ operator. The precise eigenvalue of $\mathcal{PT}$ may, however, depend on the phase assigned to $\psi_n(x)$ because $\mathcal{T}$ is an antilinear operator. Let us first investigate the phase conventions used in Fig. 2, where the real and imaginary parts of the wave function are, alternatingly, even and odd under parity as we proceed to higher excited states. The appropriate eigenvalues are thus

$$\mathcal{PT}\psi_n(x) = \psi_n^*(x) = (-1)^n\,\psi(x)\,. \tag{13}$$

In this convention, the real and imaginary parts of the eigenfunctions are alternatingly even and odd, as we would expect for anharmonic oscillators [1, 2].

However, we may simply adjust the phase of the eigenstates as follows,

$$\mathcal{PT}[(-\mathrm{i})^n\,\psi_n(x)] = \mathrm{i}^n\,\psi_n^*(x) = [(-\mathrm{i})^n\,\psi(x)]\,, \tag{14}$$

and so the wave functions $[(-\mathrm{i})^n\psi_n(x)]$, which we might just as well denote by $\psi_n(x)$, are eigenstates of H_3 and eigenstates of $\mathcal{PT}$with eigenvalue +1 [cf. Eq. (5) of Ref. [24]]. With reference to Fig. 5, let us now define the functions $\Psi_n(x) = (-\mathrm{i})^n\psi_n(x)$ as the new eigenfunctions. In the space of the Ψ_n, the conserved scalar product (4) then becomes

$$\begin{aligned}\langle\Psi_n|\Psi_m\rangle_* &= \int \mathrm{d}x\,\Psi_n^*(x)\mathcal{P}\Psi_m(x)\\ &= \int \mathrm{d}x\,\left(\mathcal{PT}\Psi_n\right)(x)\,\Psi_m(x)\\ &= \int \mathrm{d}x\,\Psi_n(x)\,\Psi_m(x)\,,\end{aligned} \tag{15}$$

where the last line is *without* complex conjugation. This latter formula shows that within the space of eigenstates, the conserved scalar product for the $\mathcal{PT}$-symmetric imaginary cubic perturbation is equal to the so-called generalized inner product for complex-scaled Hamiltonians as defined in Eq. (2.4.2) of Ref. [25], which avoids the complex conjugation of the first argument. Also, the integrand in Eq. (15) is "local" in the sense that it depends only on function values of argument x, not $-x$.

We thus identify the $\mathcal{PT}$-symmetric scalar product as the generalized inner product for complex-scaled Hamiltonians (which otherwise give rise to resonances (see Refs. [5, 6, 25]). For a "real" cubic perturbation $G\,x^3$ instead of an imaginary cubic perturbation $\mathrm{i}\,G\,x^3$, the generalized inner product describes the orthogonality properties of resonance wave functions. [4, 25], corresponding to the manifestly complex resonance energies [5, 6].

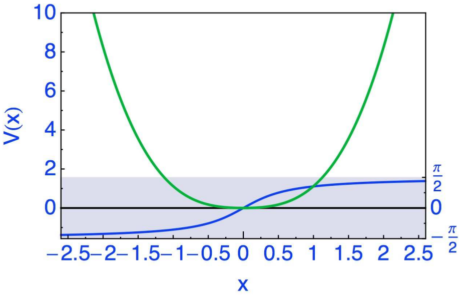

FIG. 3: (Color online.) Modulus–phase plot of the harmonic+cubic potential given in Eq. (5a). The modulus $V(x) = |W(x)| = \sqrt{\frac{1}{4}\,x^4 + G^2\,x^6}$ leads to a confining mechanism for $x \to \pm\infty$. The value of G in the plot is $G = 1.0$. The shaded area displays the complex phase of the potential and covers the interval $(-\pi/2, \pi/2)$.

IV. VISUALIZATION OF $\mathcal{PT}$–SYMMETRIC EIGENSTATES

Because the energy eigenvalues of the *imaginary* cubic oscillator (2) are real, we can associate the imaginary cubic perturbation with the *real*, "confining" quartic potential of the quartic oscillator given in Eq. (1). In the latter case, the wave functions are known to be "confined" to the "classically allowed" region where $E > V(x)$. Furthermore, from the investigations [5, 6, 10], we know that a dispersion relation connects the energy levels of the imaginary cubic perturbation $\mathrm{i}\,G\,x^3$ to the "real" cubic perturbation $G\,x^3$. However, the eigenenergies of the *imaginary* cubic potential are *real*, whereas the resonance and antiresonance energies of the *real* cubic perturbation are *complex* [4]. At some risk to oversimplification, we can say that the role of the stable quartic perturbation $+g\,x^4$ in Eq. (1) is taken over by the imaginary cubic perturbation $\mathrm{i}\,G\,x^3$, whereas the role of the unstable quartic perturbation $-g\,x^4$ is played by the real cubic perturbation $G\,x^3$ (here, we assume $g > 0$ and $G > 0$). There is no direct and obvious visualization available for the "classically allowed" region in an imaginary cubic potential. One may therefore ask in which sense the imaginary cubic perturbation "confines" the eigenstate wave functions to a "classically allowed" region of space, in particular, because the set of complex numbers $\mathbb{C}$ cannot be ordered.

An intuitive understanding can be obtained if we interpret the potential in terms of a complex modulus and a phase, which according to Eq. (5a) reads as

$$W(x) = \frac{1}{2}\,x^2 + \mathrm{i}\,G\,x^3 = V(x)\,\mathrm{e}^{\mathrm{i}\,\arg(V(x))}\,, \tag{16a}$$

$$-\pi/2 \leq \arg(W(x)) < \pi/2\,. \tag{16b}$$

In Fig. 3, we plot the modulus of the complex potential and its complex phase.

The eigenstate wave functions are plotted in Figs. 4, 5 and 6, with the idea of writing the complex eigenstate

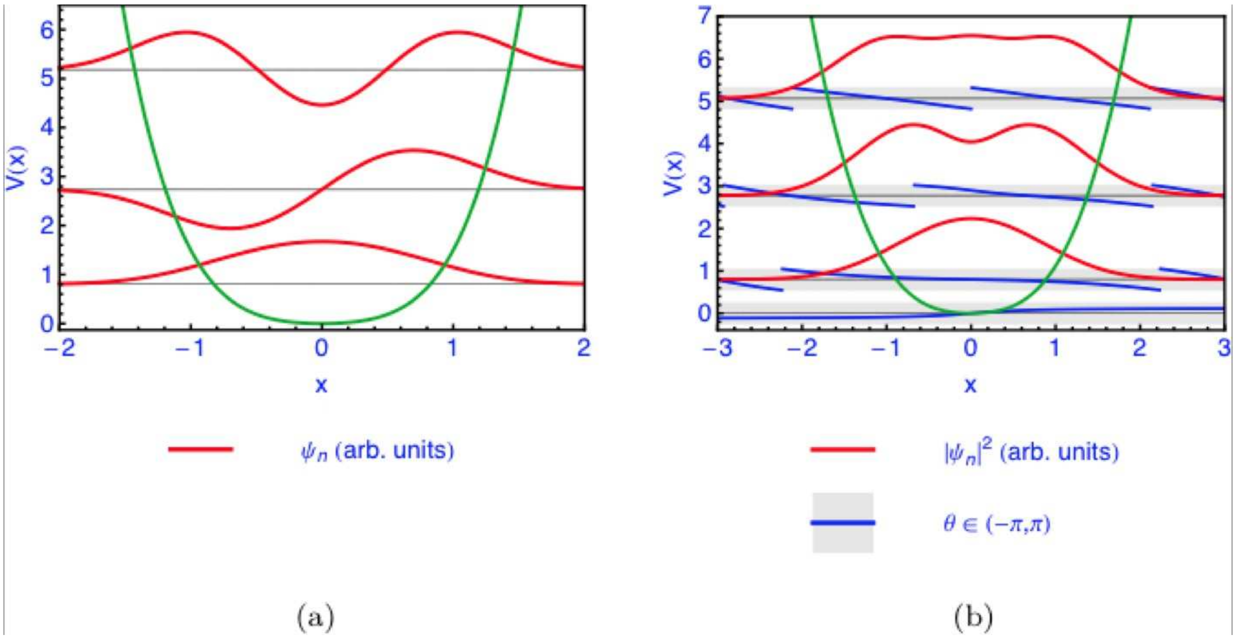

(a)

(b)

FIG. 4: (Color.) In Fig. (a), we plot the wave function of the ground and the first two excited states of the quartic oscillator. The "stable" quartic perturbation perturbs the potential in Fig. (a) and leads to a "confinement" of the wave function to the classically allowed region $E > V(x) = \frac{1}{2}x^2 + g\,x^4$. The eigenenergies of the imaginary cubic perturbation are real and allow us to plot the complex $\mathcal{PT}$-symmetric eigenfunctions in Fig. (b). For the latter, we use a modulus-phase-plot in analogy with the potential $W(x)$ displayed in Fig. 3. The complex phase of the wave function is displayed in the shaded region. The complex phase $\theta = \theta(x)$ in the decomposition $\psi_n(x) = |\psi_n(x)|\,\exp[\mathrm{i}\,\theta(x)]$ covers the interval $(-\pi, \pi)$. The red curves denote the complex modulus square of the wave functions [Figs. (a) and (b)], while the blue curves display the complex phase of the wave functions. The values of g and G in the plots read as 1.0 and 1.0, but it is useful to note that the qualitative behavior of the curves does not depend on the concrete value of g. For the $\mathcal{PT}$-symmetric potential [Fig. (b)], the quantity $|\psi_n(x)|^2$ does *not* have an interpretation as a conserved probability density, but together with the phase information, it specifies the wave function uniquely. The qualitative features ("humps") of the quartic oscillator are still present in the complex ("$\mathcal{PT}$-symmetric") domain, however the zeros of the wave functions merely become local minima. See also the following Fig. 5.

wave functions as

$$\psi_n(x) = |\psi_n(x)|\,\mathrm{e}^{\mathrm{i}\,\arg(\psi_n(x))}\,. \tag{17}$$

It is known that for Hermitian operators, the ground-state wave function always has maximum symmetry. Furthermore, for the "stable" quartic perturbation, the number of zeros of the wave function is equal to the principal quantum number. This is illustrated in Fig. 4(a). For the "unstable", "real" cubic perturbation, it has already been observed in Ref. [4] that the resonance state wave function has no zeros when considered as a complex variable (see Fig. 4 of Ref. [4]). However, a priori, this statement cannot automatically be generalized to the "stable", imaginary cubic perturbation. In Fig. 4(b), the plot of the wave function square $|\psi_n(x)|^2$ suggests that indeed, the same statement holds for the eigenstate wave functions of the imaginary cubic perturbation; they have no complex zeros. We have used a numerical value of $G = 1.0$ in Fig. 4; the ordinate axis covers the range $0 < V(x) < V_0 = 7$. In Fig. 6, we illustrate that the "confinement" mechanism holds for all values in the range $0 < G < 1$. The wave function squares are plotted in arbitrary units; in practical calculations, one normalizes to $\int \mathrm{d}x |\psi_n(x)|^2 = 1$. The complex phase of the wave function, which covers the shaded areas in Fig. 4(b), revolves in the complex plane and transits a number of Riemann sheets, i.e., it jumps from $-\pi$ to $+\pi$ several times in the interval $-3 < x < 3$.

A Wentzel–Kramers–Brioulin (WKB) analysis shows that the phase of the wave function has to behave, asymptotically, as $\arg(\psi_n(x)) \sim -x^{5/2}$ for $x \to +\infty$ and as $\arg(\psi_n(x)) \sim x^{5/2}$ for $x \to -\infty$, and we have verified this asymptotic behavior against our numerically determined wave functions. Every time the complex phase of the eigenstate wave function $\arg(\psi_n(x))$ (modulo π) attains zero, the imaginary part of the wave function vanishes, and whenever $\arg(\psi_n(x)) \bmod \pi = \pi/2$, the real part of the wave function vanishes. So, we conclude that, even for an infinitesimally small coupling G in the imaginary cubic perturbation $\mathrm{i}\,G\,x^3$, the real and imaginary parts of the wave function, individually, have an infinite number of zeros. This is somewhat surprising. E.g., the above considerations imply, among other things, that the number of complex zeros of the first-excited-state wave func-

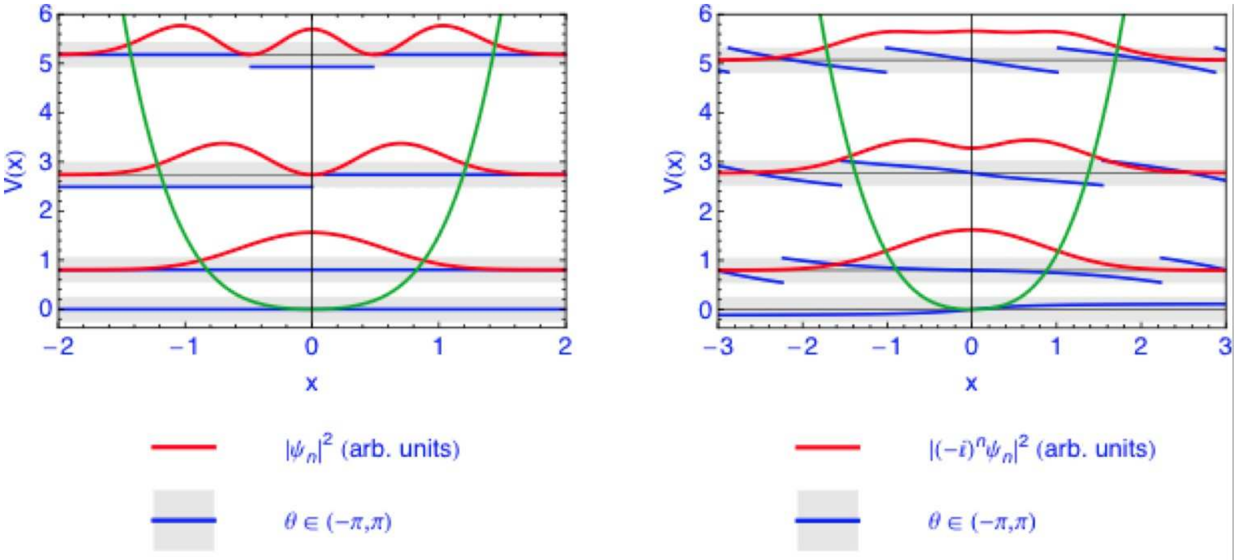

(a) (b)

FIG. 5: (Color.) In Fig. (a), we plot the probability density $\rho = |\psi(x)|^2$ of the quartic oscillator's ground state and first two excited states, in a potential $V(x) = \frac{1}{2}x^2 + g\,x^4$ with $g = 1.0$, but in a different way as compared to Fig. 4. Although the wave functions of the quartic potential are purely real, we use a complex modulus-phase plot for the real wave functions in Fig. (a). A sign change then corresponds to a jump in the complex phase from zero (for a positive real number) to $-\pi$ (for a positive negative number). In Fig. (b), we give a modulus-phase plot of the eigenstate wave functions of the imaginary cubic perturbation, but this time we shift the global phase of the wave function as compared to Fig. 4(b) and Fig. 2, by multiplying it with a phase factor $(-\mathrm{i})^n$ [see also the discussion surrounding Eq. (15)]. Here, the complex phase $\theta = \theta(x)$ enters the decomposition $(-\mathrm{i})^n\,\psi_n(x) = |\psi_n(x)|\,\exp[\mathrm{i}\,\theta(x)]$ and covers the interval $(-\pi, \pi)$.

tion of the imaginary cubic perturbation is discontinuous at $G = 0$. Namely, for $G = 0$, we have one complex zero (because the Hamiltonian is equal to the harmonic oscillator). For novanishing G, the total number of complex zeros of the wave function vanishes, while both real and imaginary parts of the wave function (for nonvanishing G) have an infinite number of zeros.

V. CONCLUSIONS

Let us add some concluding remarks. It has been stressed in the literature that the scalar product $\langle\psi|\mathcal{P}|\phi\rangle_*$ as defined in Eq. (4) is not positive definite. This has been used as an argument against the viability of $\mathcal{PT}$-symmetric Hamiltonians for the description of natural phenomena. However, one may counter argue that the same problem persists with regard to the relativistic Klein-Gordon equation where the time-like component of the current can become negative (see Chap. 2 of Ref. [26]). The Klein-Gordon equation is supposed describes a charged scalar field like the charged component of the Higgs (doublet) field [27] (the latter is usually assumed to vanish under a gauge transformation, and the remaining neutral component of the Higgs doublet is expanded about its vacuum expectation value). Strictly speaking, one has to reinterpret the zero component of the conserved Noether current as a charge density, not a probability density. Analogously, in the context of neutrino physics, an interpretation of the (non-positive definite) timelike component of conserved Noether current of the pseudo–Hermitian, generalized Dirac interaction density as a non-positive definite "weak-interaction density" (of the neutrino) has recently been proposed [28].

No physical system is known which is directly described by an imaginary cubic perturbation, and so the question of how to interpret the conserved density $\rho_*(x) = \psi(x)^+\mathcal{P}\psi(x) = \psi(x)^+\psi(-x)$ is perhaps not as immediate as in the other cases. In Eq. (15), we show that the integrand of the conserved current can be rewritten in terms of a "local" expression, containing only function evaluations at x, and interpreted in terms of a generalized inner product [25], which refrains from any complex conjugation under the integral sign [see Eq. (15)].

Incidentally, the reality of the eigenvalues of the imaginary cubic perturbation is somewhat tied to the discreteness of the spectrum: Namely, for $G = 0$, one starts from the unperturbed harmonic oscillator. In general, for a $\mathcal{PT}$-symmetric Hamiltonian, one can only show that if ϵ_n is an eigenvalue, so is the complex conjugate ϵ_n^*. However, if we assume that all eigenvalues are smooth functions of G in the limit $G \to 0$, without level crossings or

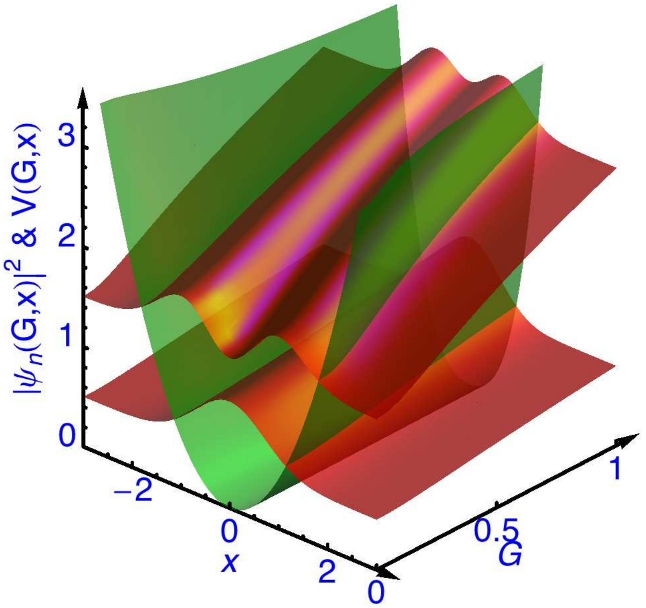

FIG. 6: (Color.) Illustration of the confinement mechanism for the imaginary cubic potential described by the Hamiltonian (2), for the ground and the first excited state. The bulk of the modulus square of the wave function is centered in the "allowed" region where the (real rather than complex) energy $E > V(x) = V(G, x) = |W(G, x)|$. The potential is plotted in green, the complex moduli of the wave functions are plotted in green. The ground state wave function has a modulus square $|\psi_0(x)|^2 = |\psi_0(G, x)|^2$ as a function of G and x. As G increases, the bound-state energy (which is equal to the base line of the wave function curve at any given value of G) increases, and the modulus of the potential forms a more narrow trough to which the ground-state wave function is confined. The same is true for the first excited state. The central minimum of the complex modulus square of the first-excited state wave function is clearly visible.

splittings or other exotic phenomena, then the reality of the eigenvalues for nonvanishing G follows immediately. The latter situation is commonly referred to as "broken" $\mathcal{PT}$-symmetry [24].

For the imaginary cubic perturbation, a "Hermitizing" transformation, which leads to an equivalent Hermitian Hamiltonian has been discussed in [24, 29, 30]. However, our discussion in Appendix A suggests that non-Hermitian time evolution operators can be useful for the description of physics phenomena in specific cases where absorption and emission phenomena have to be described. An example is given by $\mathcal{PT}$-symmetric wave guides [31–33]. Let us interpret terms in the Hamiltonian with a negative imaginary part as "absorptive" or "loss" terms and terms with a positive imaginary part as "emissive" or "gain" terms. Terms of this nature are often used in laser physics (interactions of few-level atomic systems with light fields [34]). Our discussion in Sec. IV suggests that $\mathcal{PT}$-symmetric Hamiltonians can naturally be interpreted as time-evolution operators which describe physical systems where the "emission and absorption processes are in equilibrium" (figuratively speaking) or "mutually compensate each other", and the eigenenergies of the system therefore are purely real. A typical behavior of such eigenenergies and corresponding wave functions is illustrated in Figs. 2—6. We find that the real and imaginary parts of the complex eigenstate wave functions are still eigenstates of parity, individually, even if the $\mathcal{PT}$-symmetric Hamiltonian (2) does not commute with parity. The "confining" nature of the complex modulus of the cubic anharmonic oscillator is illustrated in Fig. 3. The wave functions are concentrated in the "allowed" region with $E > V(x) = |W(x)|$, as illustrated in Figs. 4—6.

Our considerations, reported in Figs. 4—6, suggest that the eigenstate wave functions of $\mathcal{PT}$-symmetric Hamiltonians are not as "exotic" as one might otherwise imagine. An interesting observation, described in Sec. IV, is as follows: In a $\mathcal{PT}$-symmetric case, the number of zeros of the wave function cannot be used to enumerate the eigenstates. Both the real as well as the imaginary part have an infinite number of zeros, individually, but they never vanish simultaneously. The modulus of the potential, which tends to infinity as $|x| \to \infty$, is responsible for the confinement of the wave function of the imaginary cubic Hamiltonian to a "classically allowed region" $E > V(x) = |W(x)|$ (where W may be complex). Finally, we note that the field of $\mathcal{PT}$-symmetric Hamiltonians gives rise to a (still unanswered) number of theoretical questions, even if a number of the ideas used in the field have originally been formulated 70 years ago [9].

Acknowledgments

Support by the National Science Foundation (Grant PHY-1068547) and by the National Institute of Standards and Technology (Precision Measurement Grant) is gratefully acknowledged.

Appendix A: Background Information

At some risk to oversimplification, one can point out that the scientific world would be a much more interesting place if the restriction on the Hermiticity of time-evolution operators could be relaxed somehow. E.g., a complex refractive index of a material describes an absorption process in which a light wave loses intensity as it travels through a material. In 1943, Pauli introduced the idea of pseudo-Hermiticity in which the restrictions for the Hamiltonians is relaxed [9]. Pauli required that a pseudo-Hermitian operator H fulfills a relation of the form $H = \eta^{-1} H^{+} \eta$. If $\eta = \mathbb{1}$, then the Hamiltonian H is Hermitian. Along the same vein, in 1998 Bender and Boettcher proposed $\mathcal{PT}$-symmetry [3]. Existing strong numerical evidence suggests that the spectra of many typical $\mathcal{PT}$-symmetric Hamiltonians are real or come in complex conjugate pairs (the latter being referred to as "broken" $\mathcal{PT}$-symmetry). Hermiticity does not imply $\mathcal{PT}$-symmetry. The $\mathcal{PT}$-symmetric Hamiltonians constitute a new class of time-evolution operators.

Recent years have seen both $\mathcal{PT}$-symmetry and pseudo-Hermiticity gain a foothold in quantum mechanics and field theories, including the following four areas. (i) Several quantum field-theoretical models, which had been deemed problematic under the restrictions imposed by Hermiticity, were shown to be consistent under a $\mathcal{PT}$-symmetric interpretation. Notably, the *ghost* state in the Lee model was shown to have a positive norm when suitably reinterpreted [35]. (ii) In cosmological models, it is sometimes useful to write down a scalar field with negative kinetic energy. Unfortunately, this method leads to inherently unstable theories. Andrianov *et al.* [36] have studied cosmological models coupling two fields, one of which has a complex potential while both have a positive kinetic term. This model is described by a $\mathcal{PT}$symmetric Lagrangian. Furthermore, this model may help resolve a number of paradoxes in the evolution of the Universe from the big bang to the "big rip" (see Ref. [36]). (iii) The index of refraction is used to describe the propagation of light through a medium. When the medium is opaque, light is absorbed and the index of refraction becomes complex. As such, the evolution equations of certain waveguides are $\mathcal{PT}$-symmetric Schrödinger equations. One such example is a double channel waveguide, with one "loss" and one "gain" channel [32]. The "time" direction is the direction of propagation. $\mathcal{PT}$-symmetric honeycomb lattices [31] have also been studied. By introducing an alternating gain-loss structure on a hexagonal optical lattice, the dispersion relation can be tailored to be equivalent to that of tachyons [31, 37–41]. (iv) Chodos, Hauser and Kostelecky [42] have proposed a superluminal (tachyonic) model of the neutrino which leads to a natural suppression of left-handed neutrino, and right-handed anti-neutrino states. The $\mathcal{PT}$-symmetric character of the model has recently been clarified [43], and a number of "sum rules" have been found which lead to tremendous simplifications in the calculation of the tachyonic propagator [28, 44], and may even offer natural explanations for hitherto unexplained paradoxes connected to neutrino physics [28]. It should be stressed that current experimental data neither excludes nor confirms neutrino propagation exceeding the speed of light [28, 45]. Final clarification can only be obtained once more precise measurements of the neutrino propagation velocity and the beta decay endpoint spectrum are performed. The best estimates obtained from all recent measurements of the neutrino mass square using beta decay endpoints have been negative (neutrino mass square $m_\nu^2 < 0$), while still being consistent with zero within experimental error (for a list of experimental values, see Ref. [46]).

[1] A. Messiah, *Quantum Mechanics I* (North-Holland, Amsterdam, 1962).
[2] A. Messiah, *Quantum Mechanics II* (North-Holland, Amsterdam, 1962).
[3] C. M. Bender and S. Boettcher, Phys. Rev. Lett. **80**, 5243 (1998).
[4] U. D. Jentschura, A. Surzhykov, M. Lubasch, and J. Zinn-Justin, J. Phys. A **41**, 095302 (2008).
[5] U. D. Jentschura, A. Surzhykov, and J. Zinn-Justin, Phys. Rev. Lett. **102**, 011601 (2009).
[6] U. D. Jentschura, A. Surzhykov, and J. Zinn-Justin, Ann. Phys. (N.Y.) **325**, 1135 (2010).
[7] J. Zinn-Justin and U. D. Jentschura, J. Phys. A **43**, 425301 (2010).
[8] C. M. Bender, S. Boettcher, and P. N. Meisinger, J. Math. Phys. **40**, 2201 (1999).
[9] W. Pauli, Rev. Mod. Phys. **15**, 175 (1943).
[10] C. M. Bender and G. V. Dunne, J. Math. Phys. **40**, 4616 (1999).
[11] C. M. Bender and E. J. Weniger, J. Math. Phys. **42**, 2167 (2001).
[12] C. M. Bender, D. C. Brody, and H. F. Jones, Phys. Rev. Lett. **89**, 270401 (2002).
[13] C. M. Bender, K. A. Milton, and V. M. Savage, Phys. Rev. D **62**, 085001 (2000).
[14] C. M. Bender, M. V. Berry, and A. Mandilara, J. Phys. A **35**, L467 (2002).
[15] A. Mostafazadeh, J. Math. Phys. **43**, 205 (2002).
[16] A. Mostafazadeh, J. Math. Phys. **43**, 2814 (2002).
[17] A. Mostafazadeh, J. Math. Phys. **43**, 3944 (2002).
[18] A. Mostafazadeh, J. Math. Phys. **44**, 974 (2003).
[19] C. M. Bender and T. T. Wu, Phys. Rev. **184**, 1231 (1969).
[20] C. M. Bender and T. T. Wu, Phys. Rev. Lett. **27**, 461 (1971).
[21] C. M. Bender and T. T. Wu, Phys. Rev. D **7**, 1620 (1973).
[22] J. Zinn-Justin and U. D. Jentschura, Ann. Phys. (N.Y.) **313**, 197 (2004).
[23] J. Zinn-Justin and U. D. Jentschura, Ann. Phys. (N.Y.) **313**, 269 (2004).
[24] C. M. Bender, J. Brod, A. Refig, and M. E. Reuter, J. Phys. A **37**, 10139 (2004).
[25] N. Moiseyev, Phys. Rep. **302**, 211 (1998).
[26] C. Itzykson and J. B. Zuber, *Quantum Field Theory* (McGraw-Hill, New York, 1980).
[27] M. E. Peskin and D. V. Schroeder, *An Introduction to Quantum Field Theory* (Perseus, Cambridge, Massachusetts, 1995).
[28] U. D. Jentschura and B. J. Wundt, *From Generalized Dirac Equations to a Candidate for Dark Energy*, e-print arXiv:1205.0521v6, ISRN High Energy Physics, in press.
[29] C. M. Bender, P. N. Meisinger, and Q. Wang, J. Phys. A **36**, 1973 (2003).
[30] C. M. Bender, D. C. Brody, and H. F. Jones, Phys. Rev. D **70**, 025001 (2004).
[31] A. Szameit, M. C. Rechtsman, O. Bahat-Treidel, and M. Segev, Phys. Rev. A **84**, 021806(R) (2011).
[32] L. Chen, R. Li, N. Yang, D. Chen, and L. Li, arXiv:1202.2956v1 [physics.optics] (2012).
[33] D. Borisov and D. Krejčiřík, Integral Equations Operator

Theory **62**, 489 (2008).

[34] M. O. Scully and M. S. Zubairy, *Quantum Optics* (Cambridge University Press, Cambridge, UK, 1997).

[35] C. M. Bender, S. F. Brandt, J. H. Chen, and Q. Wang, Phys. Rev. D **71**, 025014 (2005).

[36] A. A. Andrianov, F. Cannata, A. Y. Kamenshchik, and D. Regoli, Int. J. Mod. Phys. D **10**, 97 (2010).

[37] O. M. P. Bilaniuk, V. K. Deshpande, and E. C. G. Sudarshan, Am. J. Phys. **30**, 718 (1962).

[38] O.-M. Bilaniuk and E. C. G. Sudarshan, Nature (London) **223**, 386 (1969).

[39] G. Feinberg, Phys. Rev. **159**, 1089 (1967).

[40] M. E. Arons and E. C. G. Saudarshan, Phys. Rev. **173**, 1622 (1968).

[41] J. Dhar and E. C. G. Saudarshan, Phys. Rev. **174**, 1808 (1968).

[42] A. Chodos, A. I. Hauser, and V. A. Kostelecky, Phys. Lett. B **150**, 431 (1985).

[43] U. D. Jentschura and B. J. Wundt, J. Phys. A **45**, 444017 (2012).

[44] U. D. Jentschura and B. J. Wundt, Eur. Phys. J. C **72**, 1894 (2012).

[45] R. Ehrlich, Astropart. Phys. **41**, 1 (2013).

[46] see the URL http://cupp.oulu.fi/neutrino/nd-mass.html.